

1 Simultaneous analysis of natural pigments and E-141i in olive oils  
2 by Liquid Chromatography–Tandem Mass Spectrometry

3

4 A. Arrizabalaga-Larrañaga<sup>(1)</sup>, P. Rodríguez<sup>(2)</sup>, M. Medina<sup>(2)</sup>, F. J. Santos<sup>(1)</sup>, E. Moyano<sup>(1)\*</sup>

5

6

7 <sup>(1)</sup> Department of Chemical Engineering and Analytical Chemistry, University of  
8 Barcelona. Av. Diagonal 645, E-08028 Barcelona, Spain

9

10 <sup>(2)</sup> Laboratori Agroalimentari, Generalitat de Catalunya, Vilassar de Mar s/n, 08348  
11 Cabrils, Spain

12

13

14

15 \* Corresponding author: Encarnación Moyano Morcillo

16

17 Department of Chemical Engineering and Analytical Chemistry  
18 University of Barcelona

19

20 Av. Diagonal 645, E-08028, Barcelona, Spain

21

22 Phone: +34-93-403-9277

23

24 E-mail: [encarna.moyano@ub.edu](mailto:encarna.moyano@ub.edu)

25 ORCID: Ane Arrizabalaga-Larrañaga (0000–0002–9379–5775)

26 Pilar Rodríguez (0000–0002–9864–1070)

27 Mireia Medina (0000–0002–7296–3514)

28 F. Javier Santos (0000–0002–8959–0363)

29 Encarnación Moyano (0000–0002–1233–8864)

30

31

32

33 **Abstract**

34 This work describes the development of an ultra-high performance liquid  
35 chromatography-tandem mass spectrometry (UHPLC-MS/MS) method for the  
36 determination of carotenoids ( $\beta$ -carotene, lutein,  $\beta$ -criptoxanthin, neoxanthin,  
37 violaxanthin) and chlorophylls, as well as their related compounds (chlorophyll A and B,  
38 pheophytin A and B and the banned dyes Cu-pyropheophytin A, Cu-pheophytin A and  
39 B) in olive oils. For this purpose, the feasibility of electrospray (ESI), atmospheric  
40 pressure chemical ionization (APCI) and atmospheric pressure photoionization (APPI)  
41 for the ionization of these compounds was evaluated and compared. Tandem mass  
42 spectrometry (MS/MS) fragmentation was discussed for each family of compounds and  
43 the most characteristic and abundant product ions were selected to propose a selective  
44 and sensitive UHPLC-MS/MS method. The best results were obtained using APCI and  
45 APPI, while ESI provided the worst signal-to-noise ratio (S/N) for all compounds. For  
46 the analysis of olive oils, a simple solid phase extraction (SPE) with silica cartridges was  
47 applied before the determination by UHPLC-MS/MS (APCI and APPI) in multiple  
48 reaction monitoring (MRM) mode. Method quality parameters were established and the  
49 results demonstrate the good performance of the new methods, providing low limits of  
50 detection (0.004 – 0.9 mg L<sup>-1</sup>), high extraction efficiencies (62 – 95%) and low matrix  
51 effects (<25%). The developed UHPLC-API-MS/MS (APCI and APPI) methods were  
52 applied to the analysis of olive oil samples and  $\beta$ -carotene, pheophytin A, pheophytin B  
53 and lutein were detected and quantified in all of them at concentrations ranging from 0.1  
54 to 9.5 mg L<sup>-1</sup>.

55 **Keywords:** Natural pigments; olive oil; atmospheric pressure chemical ionization;  
56 atmospheric pressure photoionization; ultra-high performance liquid chromatography-  
57 tandem mass spectrometry

## 58 **Introduction**

59 In the olive oil production, olives are pressed in mills to get the juice by mechanical or  
60 other physical processes that do not change the taste, smell and color of the olive oil.  
61 These procedures give rise to products known as virgin olive oil (VOO) or extra virgin  
62 olive oil (EVOO). Oils that do not achieve certain organoleptic properties are considered  
63 defective – so-called lampante oil – not suitable for human consumption without a further  
64 refining. For commercialization, this oil is refined and improved by admixing 20–30%  
65 of VOO and the resulted product is referred as olive oil (OO) [1]. Because the color is an  
66 organoleptic parameter of olive oil and one of the most important characteristics for  
67 consumers to evaluate its quality, some producers have reduced the costly addition of  
68 20-30% VOO and substituted it by the addition of a green dye to regreen the olive oil and  
69 to sell it as high quality product [2–3]. However, this practice is considered fraudulent in  
70 olive oils and their presence should be controlled.

71 Pigments such as chlorophylls and carotenoids are responsible of the olive oil color.  
72 Carotenoids present in olive oil are polyisoprenoid compounds constituted by a long alkyl  
73 chain and two cyclohexenyl rings in their structure, whereas chlorophylls are  
74 characterised by the presence of a chlorin structure (three pyrroles and one pyrroline  
75 coupled through four =CH– linkages) with a magnesium atom bonded to it (Fig. 1).  
76 Additionally, the chlorin ring can have different side chains, usually consisted in a phytol  
77 chain. These compounds are biosynthesised in nature, play an important role in the  
78 antioxidant metabolic pathways [4–6] and are unstable and sensitive to light, oxygen,  
79 acids and temperature. Due to these properties, chlorophylls are easy to degrade into  
80 pheophytins involving the release of the magnesium atom from the chlorin ring. This may  
81 occur owing to an inadequate storage or production processes of olive oil [7], resulting in  
82 color changes from green to yellow-brown [5,8]. The complexation of pheophytins

83 chlorin ring with  $\text{Cu}^{2+}$  yields the formation of green Cu-pheophytin complexes, which are  
84 much more stable and resistant to pH and temperature changes than chlorophylls due to  
85 the higher metal-chlorin ring bond energies [9]. These green copper chlorophyll  
86 complexes are commercialized as the food additive E-141i. However, although E-141i is  
87 allowed in food industry, its use in edible oils has been banned in the European Union  
88 being considered as a fraud [10].

89 Most of the published analytical methods for the determination of carotenoid and  
90 chlorophyll pigment families in olive oil matrixes are based on reversed-phase liquid  
91 chromatography (LC) [11,12]. LC columns with  $\text{C}_{30}$  stationary phases have been  
92 proposed for the analysis of carotenoids, but they provide a strong retention of the  
93 analytes especially for the most hydrophobic ones. In contrast,  $\text{C}_{18}$  columns are frequently  
94 preferred for the simultaneous analysis of chlorophylls and carotenoids, since they allow  
95 good pigment separation in shorter analysis time. In addition, UV–Vis is the detection  
96 system most commonly used for the LC analysis of chlorophylls and carotenoids, taking  
97 advantage of their chromophore groups [11,13,14]. However, the unequivocal  
98 identification and confirmation is one of the drawbacks of this methodology. Liquid  
99 chromatography coupled to mass spectrometry (LC–MS) has demonstrated to be an  
100 useful technique for the determination of these compounds in plants, grapes, wines and  
101 fruits [15–17]. Nevertheless, there are few studies for their analysis in olive oils and, most  
102 of them, are only focused on the characterization of chlorophyll [18] and Cu-chlorophyll  
103 derivative profiles [19,3] using either electrospray or atmospheric pressure chemical  
104 ionization (APCI) as ionization source. Atmospheric pressure photoionization (APPI) has  
105 also been applied in the determination of carotenoids by LC–MS but it has only been  
106 applied to standards [20]. Since, there is not any LC–MS method for the simultaneous  
107 determination of carotenoids, chlorophylls and chlorophyll derivatives in olive oil

108 samples so far, it would be interesting to evaluate the performance of different API  
109 sources for the ionization of these pigments and dyes and their applicability in the LC–  
110 MS analysis of olive oils.

111 The aim of this work was to study the ionization performance of carotenoids, chlorophylls  
112 and chlorophyll derivatives with three API sources (ESI, APCI and APPI) in order to  
113 identify which one provides the best performance. The API source selected was used to  
114 develop a new sensitive and selective ultra–high performance liquid chromatography–  
115 tandem mass spectrometry (UHPLC–MS/MS) method able to identify and quantify  
116 simultaneously natural pigments and E–141i that can be applicable to the detection of  
117 fraud in oil samples.

## 118 **Materials and methods**

### 119 **Reagents and standards**

120 Chlorophyll and carotenoid solid standards were purchased from Sigma-Aldrich  
121 (Steinheim, Germany) at purities higher than 90%. Standards of pheophytin A (PHE-A)  
122 and B (PHE-B) were obtained by acidification from their respective chlorophylls. Copper  
123 complexes of pheophytin A and B were obtained by adding an excess of copper (II) nitrate  
124 to the corresponding pheophytin. Cu-Pyropheophytin A was obtained from Cu-  
125 pheophytin A by refluxing-heating at 100° °C [21]. Chemical structures, acronyms and  
126 chemical formula of the studied compounds are shown in Fig. 1.

127 Individual stock standard solutions of chlorophylls (1,000 mg L<sup>-1</sup>) were prepared in  
128 acetone, whereas acetonitrile was used to prepare carotenoid standard solutions (500 mg  
129 L<sup>-1</sup>). An intermediate standard mixture containing all the target compounds (50 mg L<sup>-1</sup>)  
130 were prepared monthly from stock standard solutions by appropriate dilution in  
131 acetonitrile:acetone (70:30, v:v). For quantification, calibration solutions of all the

132 pigments were prepared from the intermediate standard solution at concentrations ranging  
133 from 0.04 to 15 mg L<sup>-1</sup> in acetonitrile:acetone (70:30, v:v). All these standard solutions  
134 were stored at -20°C until their use.

135 Ethanol absolute for analysis was acquired from Panreac (Barcelona, Spain). Analytical  
136 reagent grade copper nitrate was purchased from VWR (Llinars del Vallès, Barcelona,  
137 Spain). Sodium sulfate anhydrous for analysis, ≥99.0%, toluene, chlorobenzene,  
138 tetrahydrofuran, anisole, potassium hydroxide (≥85%), ammonium acetate, acetic acid (≥  
139 99.5%), hexane, acetone for pesticide residue analysis (used as extraction solvent and for  
140 mobile phase), and methanol (MeOH), acetonitrile (ACN) and water of LC–MS grade  
141 were purchased from Sigma-Aldrich (Steinheim, Germany). Solvents used as  
142 components of the mobile phase were filtered through 0.22 μm pore size Nylon  
143 membrane filters (Whatman, Clifton, NJ, USA) before their use.

144 The nitrogen (99.95%) used for the atmospheric pressure ionization (API) sources  
145 (electrospray, APCI and APPI) was purchased from Linde (Barcelona, Spain) and the  
146 high-purity argon (Ar<sub>1</sub>) (<99.999%) used as a collision-induced dissociation gas (CID  
147 gas) in the triple quadrupole instrument (QqQ) was purchased from Air Liquide (Madrid,  
148 Spain).

#### 149 **Instrumentation and UHPLC–MS/MS conditions**

150 The chromatographic separation of natural pigments and copper derivatives was  
151 performed on an UHPLC system equipped with an Accela 1250 quaternary pump, an  
152 Accela autosampler and a column oven (Thermo Fisher Scientific, San Jose, CA, USA).  
153 An Accucore C<sub>18</sub> column (100 mm × 2.1 mm id., 2.6 μm particle size) packed with  
154 superficially porous particles and purchased from Thermo Fisher Scientific was used as  
155 analytical column. The UHPLC system was coupled to a TSQ Quantum Ultra AM

156 (Thermo Fisher Scientific) mass spectrometer equipped with a triple quadrupole mass  
157 analyser. Three API sources could be swappable in the TSQ mass spectrometer, ESI,  
158 APCI and APPI (Thermo Fisher Scientific).

159 Two chromatographic separation methods were used. The first method (method 1)  
160 consisted in the separation of xanthophylls, chlorophylls and chlorophyll derivatives and  
161 the second one (method 2) for the analysis of  $\beta$ -carotene. The mobile phase of method 1  
162 consisted on water (solvent A), methanol (solvent B), acetonitrile (solvent C) and acetone  
163 (solvent D) working in a quaternary gradient elution mode. The gradient elution program  
164 started with 20% solvent A and 80% solvent C for 0.5 min followed by a linear gradient  
165 that raised up to 10% solvent B and 90% solvent C in 0.5 min. Then, this composition  
166 was kept in an isocratic step of 1.5 min. Afterwards, in a third stage, solvent D was  
167 introduced up to 50% and solvent C decreased to 50% during 1 min and these conditions  
168 were maintained in an isocratic step for 1 min. Finally, solvent D was raised up to 80%  
169 during 1 min and it was kept for 3 min more before returning to initial conditions. Method  
170 2 was based on a binary gradient elution mode consisting in acetonitrile (solvent A) and  
171 acetone (solvent B). The initial conditions were 50:50 for 2 min followed by a linear  
172 gradient elution up to 20:80% in 3 minutes. This composition was kept in an isocratic  
173 stage for 1.5min before changing to initial conditions. In both cases, the injection volume  
174 was 10  $\mu\text{L}$ , mobile phase flow-rate was 600  $\mu\text{L min}^{-1}$  and the column oven temperature  
175 was held at 25°C during the chromatographic run.

176 Ionization sources working conditions were optimized by injecting 5  $\mu\text{L}$  of a 5  $\mu\text{g mL}^{-1}$   
177 standard mixture in flow injection (FI) mode, which minimized the consumption of high  
178 cost pigment standards. The ionization source working parameters for ESI, APCI and  
179 APPI were as follow: nitrogen was used as sheath gas and auxiliary gas at flow rates of  
180 70 and 50 a.u. (arbitrary units), respectively. The ion-transfer tube temperature was held

181 at 200°C while the vaporizer temperature was set at 300°C. In the case of ESI, the  
182 electrospray needle voltage was +3 kV, whereas in APCI the corona discharge current  
183 was set at +10 kV. For APPI a krypton lamp, which emits 10.6 eV photons, was used.  
184 The tube lens potential value was optimized for each compound obtaining the best  
185 responses from 85 to 145 V, depending on the compound. Regarding APPI source, direct  
186 photoionization and dopant-assisted ionization were compared using the mobile phase  
187 composition in order to simulate the optimum conditions. Several dopants (acetone,  
188 toluene, anisole, chlorobenzene and tetrahydrofuran) were post-column added into the  
189 mobile phase using a zero-dead volume T-piece. The optimal parameters were chosen  
190 based on the signal observed for CHL-A, LUT,  $\beta$ -CRIPT and VIO in FI mode.  
191 Chlorobenzene was selected as the most appropriate dopant and the concentration that  
192 provided the best response was 5% of the total amount of mobile phase flow rate.

193

194 The mass spectral data were acquired in full scan and product ion scan modes, while for  
195 quantification multiple reaction monitoring (MRM) mode was used, operating both  
196 quadrupoles (Q1 and Q3) at a resolution of 0.7  $m/z$  full width half maximum (FWHM).  
197 In MRM, two transitions were monitored for each compound using 50 ms dwell time at  
198 1.5 mTorr argon as collision gas pressure. MRM parameters such as the optimum  
199 collision energies (CE, eV), the MRM transitions (precursor-to-product ion) and the  
200 corresponding ion ratios are given in the supporting information (Table S1). The Xcalibur  
201 software v2.1 (Thermo Fisher Scientific) was used to control the UHPLC-API-MS/MS  
202 system and to acquire and process the MS data.

## 203 **Samples**

204 Several olive oil samples were analysed to study the applicability of the developed  
205 methods. The study was carried out with twelve different commercial olive oil samples,



206 (8 OO, 2 VOO and 2 EVOO) obtained from local supermarkets (Barcelona, Spain).  
207 Additionally, a commercial E-141i dye (a mixture of Cu-chlorophyll complexes),  
208 provided by SANCOLOR S.A. company (Barcelona, Spain) was also used in this study.  
209 E-141i is a liposoluble food additive composed of copper complexes of chlorophyll  
210 derivatives. This food additive product was characterized and among the chlorophyll  
211 derivatives the most abundant were those of cu-pyropheophytin A, cu-pheophytin A and  
212 cu-pheophytin B [2]. All samples were stored in dark at ambient temperature until their  
213 analysis.

#### 214 **Sample treatment**

215 Olive oil samples were submitted to a sample treatment to obtain fat-free pigment extracts  
216 prior to their determination by UHPLC-MS/MS. For this purpose, solid phase extraction  
217 (SPE) using silica cartridges was used as first step. Briefly, pigments were extracted from  
218 olive oil samples using Supelclean™ LC-Si SPE cartridges (1.0 g, 6 mL) (Sigma-  
219 Aldrich, Steinheim, Germany) in a Visiprep System (Supelco, Bellefonte, PA, USA). SPE  
220 cartridges were first conditioned with 3 mL of hexane and afterwards 1.0 g of olive oil  
221 sample dissolved in 2 mL of hexane was loaded and passed through it. The cartridges  
222 were washed with hexane (15 mL) until total lipid removal and pigments were eluted  
223 adding acetone (5 mL). The hexane fraction, which contained lipids and the β-carotene  
224 natural pigment, was kept for further analysis, while xanthophylls, chlorophylls and  
225 chlorophyll derivatives eluted in the acetone fraction. Subsequently, on to obtain an  
226 extract of β-carotene free of lipids, the hexane fraction was saponified by adding 10 mL  
227 of a 10 % KOH in ethanol and 15 mL of water after 30 min. The hexane fraction  
228 containing the β-carotene was cleaned up three times with water and three times more  
229 with a Na<sub>2</sub>SO<sub>4</sub> aqueous solution. Both acetone (xanthophylls, chlorophylls and  
230 chlorophyll derivatives) and hexane (β-carotene after saponification) fractions were

231 evaporated until dryness under a nitrogen stream at room temperature and re-constituted  
232 in 1.5 mL of acetonitrile:acetone (70:30, v:v). The re-constituted extracts were kept frozen  
233 at -18°C in the dark to avoid any degradation, photo-oxidation, but also to facilitate the  
234 precipitation of any possible remaining lipid. Finally, the supernatant was filtered through  
235 a 0.22 µm Nylon membrane filter and 10 µL were injected into the UHPLC–MS/MS  
236 system.

## 237 **Results and discussion**

### 238 **Liquid Chromatography**

239 In this study, a reversed-phase UHPLC column packed with superficially porous particles  
240 (Accucore C<sub>18</sub>, see experimental section) was used to take advantage of the ultra-high  
241 performance provided by this column technology that should allow a high efficient  
242 chromatographic separation and short analysis time.

243 To optimize the chromatographic separation of xanthophylls, chlorophylls and  
244 chlorophyll derivatives, several mobile phase compositions and gradient elution programs  
245 were evaluated. In general, the high hydrophobicity (LogP: 8.70 – 16.53) and the low  
246 water solubility of these compounds made necessary to minimize the mobile phase water  
247 content. For this reason, the initial gradient elution program started at 20:80  
248 water:methanol (v/v) (flow rate 300 µL min<sup>-1</sup>) and it was linearly changed up to 10:90  
249 methanol:acetonitrile (v/v). Under these conditions, xanthophylls eluted at 4 times the  
250 hold-up time ( $t_M$ ) and before chlorophylls. Although some authors [11,12] used a small  
251 amount of an aqueous ammonium acetate solution at the initial conditions of the gradient  
252 elution, the substitution of this aqueous solution by just water made xanthophylls to elute  
253 earlier. This fact probably was due to the lower mobile phase ionic strength, which  
254 weakened the interaction of these analytes with the stationary phase. Additionally, the

255 coelution of neoxanthin (NEO) and violaxanthin (VIO) pigments had to be avoided, since  
256 they are isobaric compounds that also yield common product ions under tandem mass  
257 spectrometry conditions. The gradient elution program was optimized and an isocratic  
258 step of 0.5 min was necessary to achieve the separation of these compounds at base line,  
259 the final chromatographic resolution achieved was 1.9.

260 Under ternary gradient elution conditions (water:methanol:acetonitrile), chlorophylls and  
261 chlorophyll derivatives showed double chromatographic peaks. This can be attributed to  
262 the presence of epimer compounds [22] that gave the same response than the native  
263 compounds. Substituents in C-13<sub>2</sub> (methoxy group) and C-17<sub>3</sub> (phytyl group) (Fig. 1) in  
264 the epimer compounds are not in the same plane as in the native compounds. For this  
265 reason, the interaction between the stationary phase and the epimer compounds is  
266 favoured making the epimers to elute later than the native compounds. Furthermore,  
267 chlorophyll derivatives eluted in more than 25 minutes, thus it was necessary a quaternary  
268 elution program where acetone was added as the last step in order to increase the  
269 elutropic strength at the end of the chromatogram and to shorten the analysis time.  
270 Finally, to further reduce the analysis time of chlorophylls and their derivatives, mobile  
271 phase flow rate was risen up to 600  $\mu\text{L min}^{-1}$ . Fig. 2A shows the chromatogram of a  
272 natural pigment standards solution (xanthophylls, chlorophylls and chlorophyll  
273 derivatives, 2  $\mu\text{g g}^{-1}$ ) obtained under the optimum UHPLC conditions and as it can be  
274 seen, most of the compounds are separated at base line in less than 8 min, except CHL-  
275 B' and  $\beta$ -CRIPT that partially coeluted. Nevertheless, these two compounds did not show  
276 ion suppression/enhancement effect and they can be analysed individually by mass  
277 spectrometry thanks to the selection of non-interfering transitions (precursor-to-product  
278 ion). On the other hand, since  $\beta$ -carotene is a non-polar compound, mobile phase  
279 components with high elutropic strength such as acetonitrile and acetone were needed

280 to shorten the analysis time. Thereby, the obtained chromatogram for  $\beta$ -carotene is shown  
281 in Fig. 2B.

## 282 **Liquid Chromatography–Mass Spectrometry**

283 To study the atmospheric pressure ionization (API) behaviour of olive oil pigments, a  
284 standard solution (10 mg L<sup>-1</sup>) was injected in the UHPLC–MS/MS system (working  
285 conditions section 2.2) using three API sources (ESI, APCI and APPI). Upon optimizing  
286 the working parameters for each API source, it was found that vaporizer temperature and  
287 tube lens offset voltage were the most critical ones. When the vaporizer temperature was  
288 increased above 300°C, the signal of the protonated molecule ion decreased as a  
289 consequence of its fragmentation by in-source collision induced dissociation (CID), thus  
290 becoming the base peak of the mass spectrum the fragment ion originated from the loss  
291 of water (Fig. S1 for VIO). Furthermore, Fig. 3 shows the effect of tube lens voltage in  
292 the intensity of the base peak. This voltage value is compound dependent and an excessive  
293 voltage would produce the in-source CID fragmentation [23]. The highest ion intensity  
294 for chlorophylls was achieved at 140 V, while for carotenoids maximum responses were  
295 obtained at 90 V. Moreover, these compounds experimented a significant in-source CID  
296 fragmentation above this tube lens offset voltage that caused the decrease in the  
297 protonated molecule ion intensity. Besides, the high polyene conjugation and the presence  
298 of oxygen in these molecules, as well as the solvent system, have a significant influence  
299 on the stability and formation of molecular ion and protonated molecule ion. Table 1  
300 shows the ion assignment and the corresponding relative abundances observed using the  
301 three API sources (ESI, APCI and APPI with chlorobenzene) in positive ion mode.

302 Under electrospray conditions, carotenoids ( $\beta$ -CAR NEO, VIO, LUT and  $\beta$ -CRIPT)  
303 yielded the molecular ion [M]<sup>+</sup> ( $\beta$ -CAR,  $m/z$  536.5; NEO,  $m/z$  600.4; VIO,  $m/z$  600.4;

304 LUT,  $m/z$  568.4;  $\beta$ -CRIPT,  $m/z$  552.4) as base peak as well as the ion  $[M-H]^+$  (Rel. Ab.  
305 35–60%), as can be seen in Fig. 4 for LUT. These ions may be generated *via*  
306 electrochemical oxidation in the electrospray needle [24,25]. Additionally, non in-source  
307 CID fragment ions were observed at significant intensities (relative abundance < 27%)  
308 for any of these analytes, but the oxidized ion  $[M-H]^+$  showed a high tendency to generate  
309 adducts with the mobile phase components. Ions such as  $m/z$  617.4 for NEO,  $m/z$  617.4  
310 for VIO and  $m/z$  585.4 for LUT, shifted 18 units above the ion  $[M-H]^+$  and they could be  
311 assigned to the water adduct ions  $[M-H+H_2O]^+$ . Furthermore, methanol adduct ions  $[M-$   
312  $H+CH_3OH]^+$  such as  $m/z$  599.4 for LUT and  $m/z$  583.4 for  $\beta$ -CRIPT were also observed.

313 Regarding chlorophylls the ions generated by ESI include both ions  $[M+H]^+$  and  
314  $[M+Na]^+$ , being the base peaks for CHL-A and CHL-B, respectively (Fig. 4).  
315 Additionally, chlorophylls and their epimers also showed the molecular ion  $[M]^+$  as  
316 occurred with carotenoids. Under these conditions, the UHPLC–ESI–MS chromatogram  
317 showed a high background noise resulting in a low signal-to-noise ratio (S/N) for all  
318 compounds and as a consequence the limits of detection were relatively high ranging from  
319 0.8 to 3 mg L<sup>-1</sup>. Therefore, APCI and APPI were evaluated as alternatives to ESI in order  
320 to improve the signal intensity, since the gas-phase ionization mechanisms in these two  
321 API sources may be advantageous for the ionization of these highly conjugated  
322 compounds.

323 The ionization of chlorophylls and their derivatives (including epimer compounds) by  
324 APCI provided the ion  $[M+H]^+$  (CHL-A,  $m/z$  893.5; CHL-B,  $m/z$  907.5; PHE-A,  $m/z$   
325 871.5; PHE-B,  $m/z$  885.5; Cu-PHE-A,  $m/z$  932.5; Cu-PHE-B,  $m/z$  946.5; Cu-PyroPHEa,  
326  $m/z$  874.5) as base peak, as it was observed in ESI. Nevertheless, no adduct ions were  
327 generated and only a slight in-source CID fragmentation (relative abundance around  
328 25%) was observed. However, unlike in ESI, xanthophylls showed a significant in-source

329 CID fragmentation in APCI, mainly due to the loss of a water molecule providing the ion  
330  $[M+H-H_2O]^+$  (NEO,  $m/z$  583.4; VIO,  $m/z$  583.4; LUT,  $m/z$  551.4;  $\beta$ -CRIPT,  $m/z$  535.4).  
331 Nevertheless, in spite of the in-source fragmentation for xanthophylls, the ion  $[M+H]^+$   
332 continued being the base peak in the mass spectra of  $\beta$ -CAR, VIO and  $\beta$ -CRIPT. In the  
333 case of LUT and NEO, the in-source fragment ion  $[M+H-H_2O]^+$  dominated both mass  
334 spectra as a consequence of the formation of a relatively stable allylic carbocation in the  
335  $\epsilon$ -ring. As an example, Fig. 4 shows the mass spectra obtained for CHL-A and LUT in  
336 APCI.

337 Regarding APPI, both chlorophyll and carotenoid families were ionized with no need of  
338 a dopant. The direct photoionization could be due to the high number of double bonds  
339 and electron-donor methyl groups in the chemical structure of these compounds, which  
340 results in low ionization potential values [26] that could facilitate the direct  
341 photoionization. Chlorophylls and their derivatives under direct photoionization provided  
342 the ion  $[M+H]^+$  without significant in-source CID fragmentation, whereas most of  
343 carotenoids yielded the molecular ion  $[M]^+$  ( $\beta$ -CRIPT and  $\beta$ -CAR always showed the  
344 ion  $[M+H]^+$ ) and a low in-source CID fragmentation due to the loss of a water molecule.

345 Despite direct ionization occurred with these compound families, several dopants  
346 (acetone, toluene, chlorobenzene, anisole and tetrahydrofuran) were also tested in order  
347 to study their effect in the ionization efficiency to improve diagnostic ion signal. These  
348 studies were carried out using the mobile phase composition in order to simulate the  
349 optimum conditions for VIO, LUT,  $\beta$ -CRIPT and CHL-A as model compounds and the  
350 ions observed are summarized in Table S2. Among the dopants evaluated, acetone,  
351 tetrahydrofuran and toluene allowed the ionization of the analytes in the same way,  
352 providing similar mass spectral patterns. VIO,  $\beta$ -CRIPT and CHL-A yielded the ion  
353  $[M+H]^+$ , while the ion  $[M+H-H_2O]^+$  (in-source CID fragment) dominated the mass

354 spectrum of LUT. It must be noted that these dopants generally lack the capacity for  
355 charge exchange since fast self-protonation between a dopant radical ion  $[D]_{+\bullet}$  and a  
356 neutral dopant molecule  $[D]$  could be the predominant ion-molecule reaction in the gas-  
357 phase, leading to the ion corresponding to the protonated dopant  $[D+H]_{+}$ . Afterwards, the  
358 analyte would be ionized *via* proton-transfer reactions to yield the ion  $[M+H]_{+}$ . However,  
359 anisole and chlorobenzene dopants could favour the charge exchange between the dopant  
360 molecular ion  $[D]_{+\bullet}$  and the neutral analyte molecule  $[M]$  to yield the analyte molecular  
361 ion  $[M]_{+\bullet}$ . No in-source CID fragmentation occurred for carotenoids and only for LUT  
362 (Fig. 4) some fragment ions were observed at low relative abundance (<18%).  
363 Nevertheless, in the case of CHL-A (Fig. 4), in addition to the molecular ion  $[M]_{+\bullet}$ ,  
364 proton-transfer reactions also occurred to yield the ion  $[M+H]_{+}$ . The analyte responses  
365 observed when working in both direct and dopant-assisted APPI modes were normalized  
366 to the highest signal for each compound in each case (Fig. S2). Generally, the highest  
367 relative signal intensity was obtained using chlorobenzene as dopant; although for LUT,  
368 the response was slightly higher using anisole. As a compromise, chlorobenzene was  
369 selected as the most suitable dopant for the APPI of the target compounds. Finally, Fig.  
370 5 shows the comparison of the relative signal intensity of the base peak normalized to  
371 each compound in each ionization source (ESI, APCI and chlorobenzene assisted APPI).  
372 As can be observed, ESI shows the lowest response in all cases, so it was discarded for  
373 further studies. Although APPI provided the best results, APCI could also be considered  
374 as a good alternative for the analysis of these compounds since for most of them the  
375 response was only slightly lower than that obtained in APPI.

376 To improve the detectability, the sensitivity and to ensure the identification and  
377 quantitative determination of target compounds, tandem mass spectrometry was  
378 evaluated. The assignments of the main product ions are summarized in Table 2. Tandem

379 mass spectra of chlorophylls and carotenoids ions generated by APCI and APPI were  
380 studied. The corresponding product ions were characterized and the two most selective  
381 and abundant ones were selected for quantitative and confirmatory purposes when  
382 working in multiple reaction monitoring (MRM) mode. The product ion scan of  
383 chlorophylls and carotenoids were acquired at collision energies between 5 eV and 50  
384 eV. The collision energies and the selected precursor and product ions as well as the ion  
385 ratios calculated for each compound are given in the supporting information (Table S1).

386 In the case of chlorophylls and their copper derivatives, the product ion scan for the  
387 precursor ion  $[M+H]^+$  was obtained using an isolation window of 10  $m/z$  in order to  
388 preserve the isotopic information of the product ions. Instead, for pheophytins, a standard  
389 isolation window of 1  $m/z$  was used. Thereby, it was possible to confirm that all the  
390 product ions observed for chlorophylls and their copper derivatives kept the metal atom  
391 in their chemical structure (Fig. S3). Moreover, the fragmentation pattern of the  
392 chlorophyll family was characterized by the loss of the phytol chain 278 Da ( $C_{20}H_{38}$ ) and  
393 the consecutive cleavage of the carboxymethyl ester (60 Da,  $C_2H_4O_2$ ) at C-13<sub>2</sub> yielding  
394 the ion  $[M+H-C_{22}H_{42}O_2]^+$ , except for Cu-pyropheophytin A which lacked the  $\beta$ -keto  
395 ester. In addition, Cu-pyropheophytin A also showed product ions due to the carboxy-  
396 phytol loss ( $m/z$  552,  $[C_{32}H_{32}CuN_4O]^+$ ) and the cleavage at C-17<sub>3</sub> to lose  $CH_2CH_2COO$ -  
397 phytol ( $m/z$  522,  $[C_{30}H_{27}CuN_4O]^+$ ). Regarding chlorophyll epimers, the CID  
398 fragmentation behaviour is slightly different, even the similarity of the product ions  
399 observed, the relative abundances are quite different at the same collision energy. This  
400 fact could be explained because of the activation energy needed to fragment the epimer  
401 compound is lower than that required for the native compound, which could be related  
402 with the relative position of C-13<sub>2</sub> and C-17<sub>3</sub> (Fig. S4) that seems to stabilize the  
403 chemical structure in the case of the native compound.



404 Regarding carotenoids, the base peak ions observed in APCI and APPI were selected as  
405 precursor ions in tandem mass spectrometry. In all cases, the high polyene conjugation  
406 and the hydroxyl group in the chemical structure of xanthophylls were involved in the  
407 formation of the main characteristic and common product ions. A general fragmentation  
408 pattern consisting in consecutive losses shifted 14 Da ( $\text{CH}_2$ ) and 28 Da ( $\text{CH}_2=\text{CH}_2$ ) was  
409 observed as a result of the typical fragmentation of alkene chains. Additionally, product  
410 ions generated by dehydroxylation (loss of OH) or dehydration (loss of  $\text{H}_2\text{O}$ ) from the  
411 respective precursor ion were also observed for all xanthophylls in both APCI and APPI.

412 For LUT the precursor ion was different in both APCI and APPI, but the two most  
413 abundant product ions observed, such as the ions at  $m/z$  145 [ $\text{C}_{11}\text{H}_{13}$ ] $^+$  and  $m/z$  119  
414 [ $\text{C}_9\text{H}_{11}$ ] $^+$ , were the same in both API sources. Moreover, the ion [ $\text{C}_9\text{H}_{11}$ ] $^+$  ( $m/z$  119) was  
415 the base peak in the product ion spectra of hydroxy carotenoids ( $\beta$ -CRIPT and LUT)  
416 although it was also observed with lower intensity (40%) in the product ion spectra of  $\beta$ -  
417 CAR, VIO and NEO with both API sources. Besides, the common product ion [ $\text{C}_{11}\text{H}_{13}$ ] $^+$   
418 ( $m/z$  145) was also observed using APPI for all xanthophylls. Furthermore, both VIO and  
419 NEO have a cyclohexyl ring with an epoxide and an hydroxyl group which are involved  
420 in the formation of product ion at  $m/z$  221 [ $\text{C}_{14}\text{H}_{21}\text{O}_2$ ] $^+$  in APCI due to the loss of 380 Da.

421 Once the MS/MS conditions were established for each compound and the MRM  
422 transitions for quantification and confirmation (Table S1) purposes were selected, the  
423 performance of the UHPLC-MS/MS methods were evaluated using both APCI and APPI  
424 sources. Instrumental limit of detection (ILOD) and limit of quantitation (ILOQ) were  
425 calculated using standard solutions (Table 3). LODs based on a signal-to-noise ratio of  
426 3:1 and LOQs based on a signal-to-noise ratio of 10:1 were determined by injecting 10  
427  $\mu\text{L}$  of standard solutions at low concentration levels. As can be seen, similar LODs values  
428 were obtained in both APCI and APPI except for LUT and VIO that showed slightly

429 better sensitivity in APCI. Nevertheless, LOD values were always lower than 0.2 mg L<sup>-1</sup>  
430 and down to 0.003 mg L<sup>-1</sup> for the best cases. Besides, chlorophyll derivative values were  
431 expected to be similar to the ones determined for their corresponding native compounds.  
432 Considering that most of the natural pigments are usually expected at mg L<sup>-1</sup> in olive oil,  
433 these ILODs can be enough to detect and determine these compounds in the final olive  
434 oil extracts.

### 435 **Sample analysis**

436 The application of the developed UHPLC-API-MS/MS methods for the determination  
437 of pigments in olive oil samples required a previous sample treatment (extraction and  
438 clean up) in order to achieve extracts clean enough before their analysis by UHPLC-  
439 MS/MS. In this work, a SPE method using silica cartridges was applied as sample  
440 treatment before the chromatographic analysis of natural pigments in olive oils. Acetone  
441 extract contained the chlorophylls, chlorophyll derivatives and xantophylls, while the  
442 saponified hexane extract contained the  $\beta$ -carotene.

443 Due to the lack of an olive oil sample free of target pigments, an olive oil sample (OO-  
444 S8) spiked with target compounds at 4 mg L<sup>-1</sup> (4 times higher than the endogenous  
445 concentration determined in this sample) was used for the optimization of working  
446 conditions and the estimation of quality parameters of the method. Olive oil sample and  
447 a spiked olive oil sample were submitted to the sample treatment procedure and the  
448 corresponding extracts were analysed by UHPLC-API-MS/MS in order to calculate the  
449 SPE extraction efficiency (EE, %). Additionally, an aliquot of the olive oil sample extract  
450 was also spiked with standards (4 mg L<sup>-1</sup>) to evaluate the matrix effect (ME, %) in the  
451 ionization by comparing it with the corresponding response of the standard at the same  
452 concentration level. For most compounds, the SPE EE% ranged from 88% to 95% with  
453 RSD% lower than 10%. Only CHL-A showed a lower EE% value (63%) owing to a

454 possible degradation of the added pigment into pheophytin due to the own acidity of the  
455 oil sample. ME (%) values ranged from 8% to 25% with RSD% values lower than 15%,  
456 which indicated that both APCI and APPI methods only showed a slightly matrix effect.  
457 This low ME% allowed us to use the external calibration method for the quantitative  
458 analysis of these compounds in olive oil samples. Moreover, method limits of  
459 quantification (MLOQs), defined as S/N of 10, ranged between 0.036 and 0.80 mg L<sup>-1</sup>  
460 (Table 3). The linearity was satisfactory for all compounds within the concentration  
461 working range studied (0.04 – 15 mg L<sup>-1</sup>), showing linear regression coefficients (R<sup>2</sup>)  
462 higher than 0.998. In addition, run-to-run precision was estimated (concentration level ~  
463 4 mg L<sup>-1</sup>) obtaining relative standard deviation values (n = 3, RSD%) lower than 7% in  
464 all cases. Trueness was also evaluated obtaining satisfactory results, with relative errors  
465 lower than 10%. These results show that the two UHPLC–API–MS/MS methods provide  
466 good performance and both could be proposed for the analysis of carotenoid and  
467 chlorophyll pigments, although APCI should be used if extra sensitivity is required, since  
468 APCI showed slightly better LODs than APPI. To our knowledge, there are no data  
469 published on UHPLC–MS/MS using APCI or APPI for the simultaneous determination  
470 of carotenoids, chlorophylls and the chlorophyll copper potential adulterant (E–141i) in  
471 olive oil samples.

472 In this work, in order to evaluate the feasibility of the developed SPE UHPLC–API–  
473 MS/MS methods a total of 12 olive oil samples were analysed in triplicate (n=3). Among  
474 the olive oil samples analysed, copper chlorophyll complexes were not detected, thus,  
475 indicating that all these selected samples were not adulterated with E–141i green dye.  
476 Moreover, neither  $\beta$ –CRIPT nor NEO were detected above their MLOQ using both APCI  
477 and APPI sources. Besides,  $\beta$ –CAR, PHE-A, PHE-B and LUT were quantified in all  
478 samples at concentration levels ranging from 0.1 to 9.5 mg L<sup>-1</sup> (Fig. 6). Moreover, VIO,

479 was identified in all samples, although only in VOO and EVOO samples the concentration  
480 was above the MLOQ using both methods. However, VIO was not detected in OO  
481 samples with APPI method, but the better sensitivity of APCI allowed its detection at  
482 concentration levels close to MLOQ. As can be seen in Fig. 6, the results obtained with  
483 the proposed SPE UHPLC–MS/MS methods with APCI and APPI agreed.

484 For confirmatory purposes and for avoiding false positives, ion ratios between both  
485 quantitative and confirmatory transitions peak areas were compared with that obtained  
486 from the corresponding standards. For all the compounds detected in samples above the  
487 MLOQ, the ion ratio deviation ranged from 0.1 to 10% indicating the absence of false  
488 positive among the analysed samples.

489 Finally, since there was not any adulterated sample with E–141i, in order to test the  
490 feasibility of the method proposed for the analysis of Cu-chlorophyll complexes, two OO  
491 samples (OO-S2 and OO-S7) were spiked with E–141i to achieve low concentration  
492 levels on copper chlorophyll derivatives ( $0.09 - 0.16 \text{ mg L}^{-1}$ ) based in data found in the  
493 literature about its use in fraud practices [3]. These samples were submitted to the  
494 developed SPE UHPLC–API–MS/MS (APCI, APPI) methods. Both methods provided  
495 similar results (trueness 7-10%, RSD% 4-6%), demonstrating that both methods were  
496 able to detect and quantify these copper derivatives in olive oil samples. As an example,  
497 Fig. 7 shows the SPE UHPLC–APCI–MS/MS chromatograms obtained for (A)  
498 quantitation and (B) confirmation transitions in sample OO-S7 spiked with E–141i at  $0.16$   
499  $\text{mg L}^{-1}$ .

## 500 **Conclusions**

501 UHPLC–MS/MS using APCI and APPI sources has proved to be reliable and accurate  
502 method for the determination of carotenoids, chlorophylls and chlorophyll derivatives in

503 olive oils. The use of an UHPLC reversed-phase column (Accucore C18) and a quaternary  
504 gradient elution (water:methanol:acetonitrile:acetone) provided efficient  
505 chromatographic separation and resolution of all target compounds in a short analysis  
506 time (< 8 min). Furthermore, the results obtained in the ionization behaviour and MS/MS  
507 fragmentation studies showed that best ionization efficiencies were achieved using both  
508 APCI and APPI, being the predominant ions the protonated molecule  $[M+H]^+$  for  
509 chlorophylls and their derivatives and the ions  $[M+H]^+$ ,  $[M+H-H_2O]^+$  and  $[M]^{+\bullet}$  for  
510 carotenoids. Chlorophylls showed a common MS/MS fragmentation pattern based on the  
511 loss of the phytyl chain (278 Da;  $C_{20}H_{38}$ ) and the consecutive cleavage of the  
512 carboxymethyl ester (60 Da,  $C_{22}H_{42}O_2$ ) at C-132. While for carotenoids, the main product  
513 ions aroused from the fragmentation of the high polyene conjugated chain and the  
514 hydroxyl group. The combination of a simple SPE method and gas-phase ionization  
515 sources (APCI and APPI) allowed to keep the matrix effect under control, lower than  
516 25%, and to use external calibration method for quantitative analysis. The good  
517 performances of the developed methods and the suitable results obtained in the analysis  
518 of olive oil samples have demonstrated their applicability and they can be proposed for  
519 the determination of the pigment profile as well as the detection of possible exogenous  
520 adulterants.

521

## 522 **Funding information**

523 The authors gratefully acknowledge the financial support received from Spanish Ministry  
524 of Economy and Competitiveness under the project CTQ2015-63968-C2-P and from the  
525 Agency for Management of University and Research Grants (Government of Catalonia,  
526 Spain) under the project 2017SGR-310. Ane Arrizabalaga Larrañaga also thanks the

527 Agency for Management of University and Research Grants (Government of Catalonia)  
528 and to the European Social Fund for the PhD FI–DGR fellowship.

## 529 **Compliance with ethical standards**

530 **Conflict of interest** The authors declare that they have no conflicts of interest.

531

## 532 **References**

533 [1] International Olive Oil Council, RES-2/91-IV-04, Trade Standard Applying to table  
534 olives, 2004.

535 [2] Roca M, Gallardo-Guerrero L, Mínguez-Mosquera MI, Rojas BG. Control of olive  
536 oil adulteration with copper-chlorophyll derivatives. *J. Agric. Food Chem.* 2010;  
537 58: 51–56.

538 [3] Fang M, Tsai CF, Wu GY, Tseng SH, Cheng HF, Kuo CH, Hsu CL, Kao YM, Shih  
539 DYC, Chiang YM. Identification and quantification of Cu-chlorophyll adulteration  
540 of edible oils. *Food Addit. Contam. Part B.* 2015; 8: 157–162.

541 [4] Luaces P, Pérez AG, García JM, Sanz C. Effects of heat-treatments of olive fruit on  
542 pigment composition of virgin olive oil. *Food Chem.* 2015; 90: 169–174.

543 [5] Buckle KA, Edwards RA. Chlorophyll, colour and pH changes H.T.S.T. processed  
544 green pea puree. *J. Food Technol.* 1970; 5: 173–186.

545 [6] Demmig-Adams B, Gilmore AM, Adams WW. In vivo functions of carotenoids in  
546 higher plants. *Faseb. J.* 1996; 10: 403–412.

547 [7] Mangos TJ, Berger RG. Determination of major chlorophyll degradation products.  
548 *Z. Leb. Unters Forsch A.* 1997; 204: 345–350.

549 [8] Weemaes CA, Ooms V, Van Loey AM, Hendrickx ME. Kinetics of chlorophyll

- 550 degradation and color loss in heated broccoli juice. *J. Agric. Food Chem.* 1999; 47:  
551 2404–2409.
- 552 [9] Jones ID, White RC, Gibbs E, Butler LS, Nelson LA. Experimental Formation of  
553 Zinc and Copper Complexes of Chlorophyll Derivatives in Vegetable Tissue by  
554 Thermal Processing. *J. Agric. Food Chem.* 1977; 25: 149–153.
- 555 [10] Council Decision (EU) 1333/2008 of 16 December 2008 on food additives. *Off. J.*  
556 *Eur. Communities. L* 354, 2008, 1-342.
- 557 [11] Mínguez-Mosquera MI, Gandul-Rojas B, Gallardo-Guerrero ML. Rapid method of  
558 quantification of chlorophylls and carotenoids in virgin olive oil by high-  
559 performance liquid chromatography. *J. Agric. Food Chem.* 1992; 40: 60–63.
- 560 [12] Mateos R, García-Mesa JA. Rapid and quantitative extraction method for the  
561 determination of chlorophylls and carotenoids in olive oil by high-performance  
562 liquid chromatography. *Anal. Bioanal. Chem.* 2006; 385: 1247–1254.
- 563 [13] Giuffrida D, Salvo F, Salvo A, La Pera L, Dugo G. Pigments composition in  
564 monovarietal virgin olive oils from various sicilian olive varieties. *Food Chem.*  
565 2007; 101: 833–837.
- 566 [14] Criado MN, Romero MP, Motilva MJ. Effect of the technological and agronomical  
567 factors on pigment transfer during olive oil extraction. *J. Agric. Food Chem.* 2007;  
568 55: 5681–5688.
- 569 [15] Kao TH, Huang SC, Inbaraj BS, Chen BH. Determination of flavonoids and  
570 saponins in *Gynostemma pentaphyllum* (Thunb.) Makino by liquid  
571 chromatography-mass spectrometry. *Anal. Chim. Acta.* 2008; 626: 200–211.

- 572 [16] Mendes-Pinto MM, Silva Ferreira AC, Caris-Veyrat C, De Pinho PG. Carotenoid,  
573 chlorophyll, and chlorophyll-derived compounds in grapes and port wines. J. Agric.  
574 Food Chem. 2005; 53: 10034–10041.
- 575 [17] De Rosso VV, Mercadante AZ. Identification and quantification of carotenoids, by  
576 HPLC-PDA-MS/MS, from Amazonian fruits. J. Agric. Food Chem. 2007; 55:  
577 5062–5072.
- 578 [18] Aparicio-Ruiz R, Riedl KM, Schwartz SJ. Identification and quantification of  
579 metallo-chlorophyll complexes in bright green table olives by high-performance  
580 liquid chromatography-mass spectrometry quadrupole/time-of-flight. J. Agric.  
581 Food Chem. 2011; 59: 11100–11108.
- 582 [19] Zvezdanovic JB, Petrovic SM, Markovic DZ, Andjelkovic TD, Andjelkovic DH.  
583 Electrospray ionization mass spectrometry combined with ultra high performance  
584 liquid chromatography in the analysis of *in vitro* formation of chlorophyll  
585 complexes with copper and zinc. J. Serb. Chem. Soc. 2014; 79: 689–706.
- 586 [20] Rivera SM, Christou P, Canela-Garayoa R. Identification of carotenoids using mass  
587 spectrometry. Mass Spectrom. Rev. 2014; 33: 353–372.
- 588 [21] Schwartz SJ, Woo SL, von Elbe JH. High-performance liquid chromatography of  
589 chlorophylls and their derivatives in fresh and processed spinach. J. Agric. Food  
590 Chem. 1981; 29: 533–535.
- 591 [22] Kuronen P, Hyvärinen K, Hynninen PH, Kilpeläinen I. High-performance liquid  
592 chromatographic separation and isolation of the methanolic allomerization products  
593 of chlorophyll a. J. Chromatogr. A. 1993; 654: 93–104.
- 594 [23] Gross JH, Eckert A, Sierbert W. Negative-ion electrospray mass spectrometry of



595 carbon dioxide-protected N-heterocyclic anions. *J. Mass Spectrom.* 2002; 37: 541–  
596 643.

597 [24] Liu D, Gao Y, Kispert LD. Electrochemical properties of natural carotenoids. *J.*  
598 *Electroanal. Chem.* 2000; 488: 140–150.

599 [25] Cole RB (ed.), *Electrospray and MALDI mass spectrometry: fundamentals,*  
600 *instrumentation, practicalities, and biological applications*, second ed., Wiley, New  
601 York, 2010.

602 [26] Nakato Y, Chiyoda T, Tsubomura H. Experimental determination of Ionization  
603 Potentials of Organic Amines, b-Carotene and Chlorophyll a. *Bull. Chem. Soc. Jpn.*  
604 1974; 47: 3001–3005.

605

606 **Figure Captions**

607 **Fig. 1** Chemical structures of studied natural pigments.

608 **Fig. 2** UHPLC–APCI–MS/MS chromatogram obtained from standard mixtures of target  
609 compounds at a concentration of 2 mg L<sup>-1</sup>. Chromatogram A: method 1;  
610 chromatogram B: method 2. Compounds: (1) NEO; (2) VIO; (2') VIO'; (3) LUT;  
611 (3') LUT'; (4) CHL-B; (4') CHL-B'; (5) β-CRIPT; (6) CHL-A; (6') CHL-A'; (7)  
612 PHE-B; (8) Cu–PHE-B; (9) PHE-A; (9') PHE-A'; (10) Cu–PHE-A; (10') Cu–  
613 PHE-A'; (11) Cu–PyroPHE-A; (12) β-CAR.

614 **Fig. 3** Effect of tube lens offset voltage on carotenoids and chlorophylls response in  
615 APCI. Mass spectra of β-CRIPT (left) at a tube lens voltage of 90 V (up) and 140  
616 V (bottom) and of Cu-PHE-A (right) at a voltage of 140 V (up) and 190 V  
617 (bottom).

618 **Fig. 4** ESI, APCI and APPI (5% chlorobenzene as dopant) mass spectra of LUT and  
619 CHL-A in positive-ion mode.

620 **Fig. 5** Comparison of target compounds responses (normalized chromatographic peak  
621 height) using ESI, APCI and APPI (chlorobenzene as dopant) as ionization  
622 sources.

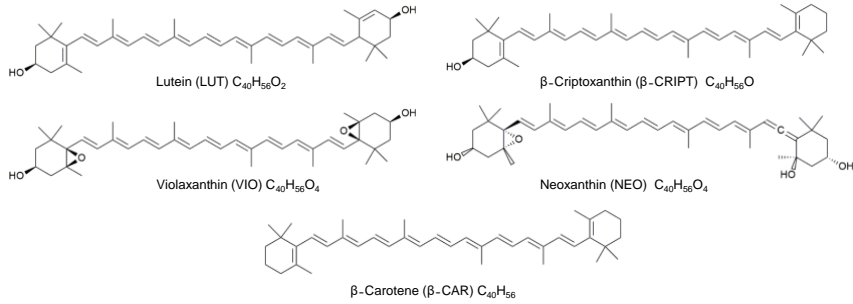
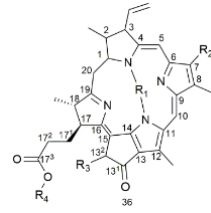
623 **Fig. 6** Individual concentrations of β-CAR, PHE-A, PHE-B and LUT for edible oils  
624 obtained by UHPLC–APCI–MS/MS and UHPLC–APPI–MS/MS methods.

625 **Fig. 7** UHPLC–APCI–MS/MS chromatogram obtained for (A) quantitation and (B)  
626 confirmation transitions from the analysis OO-S7 sample spiked with E-141i at  
627 0.16 mg L<sup>-1</sup>.

628

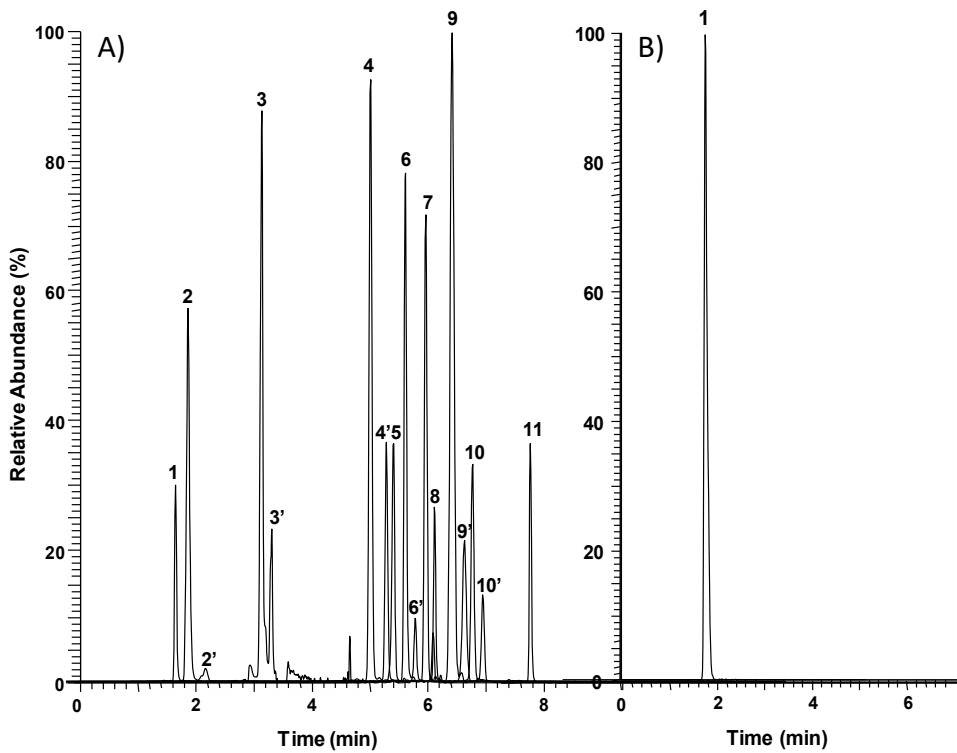
629 Figure 1:

	R <sub>1</sub>	R <sub>2</sub>	R <sub>3</sub>	R <sub>4</sub>	Formula
CHL-A	Mg	CH <sub>3</sub>	CH <sub>3</sub> COOH	C <sub>20</sub> H <sub>39</sub>	C <sub>55</sub> H <sub>72</sub> MgN <sub>4</sub> O <sub>5</sub>
CHL-B	Mg	CHO	CH <sub>3</sub> COOH	C <sub>20</sub> H <sub>39</sub>	C <sub>55</sub> H <sub>70</sub> MgN <sub>4</sub> O <sub>6</sub>
PHE-A	H <sub>2</sub>	CH <sub>3</sub>	CH <sub>3</sub> COOH	C <sub>20</sub> H <sub>39</sub>	C <sub>55</sub> H <sub>74</sub> N <sub>4</sub> O <sub>5</sub>
PHE-B	H <sub>2</sub>	CHO	CH <sub>3</sub> COOH	C <sub>20</sub> H <sub>39</sub>	C <sub>55</sub> H <sub>72</sub> N <sub>4</sub> O <sub>6</sub>
Cu-PHE-A	Cu	CH <sub>3</sub>	CH <sub>3</sub> COOH	C <sub>20</sub> H <sub>39</sub>	C <sub>55</sub> H <sub>72</sub> CuN <sub>4</sub> O <sub>5</sub>
Cu-PHE-B	Cu	CHO	CH <sub>3</sub> COOH	C <sub>20</sub> H <sub>39</sub>	C <sub>55</sub> H <sub>70</sub> CuN <sub>4</sub> O <sub>6</sub>
Cu-PyroPHE-A	Cu	CH <sub>3</sub>	3H	C <sub>20</sub> H <sub>39</sub>	C <sub>55</sub> H <sub>71</sub> CuN <sub>4</sub> O <sub>3</sub>



630

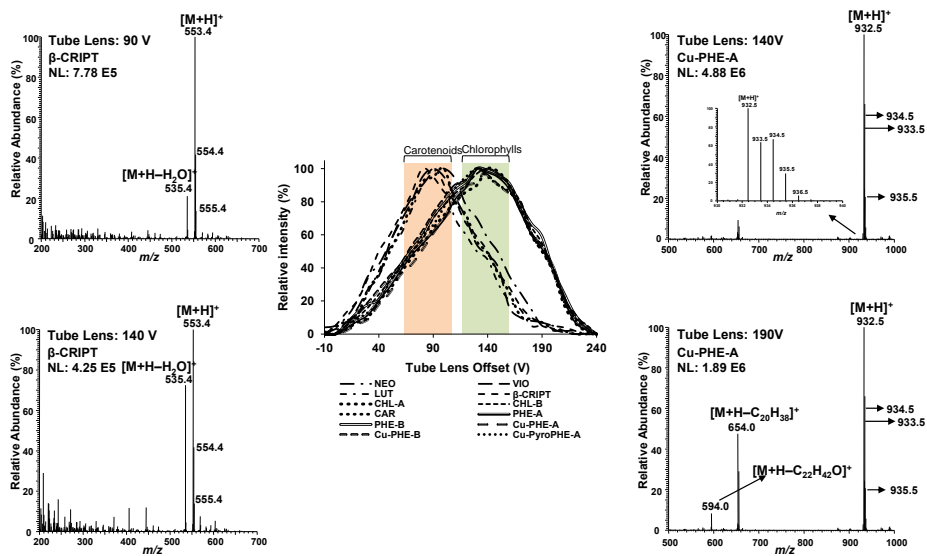
631 Figure 2:



632

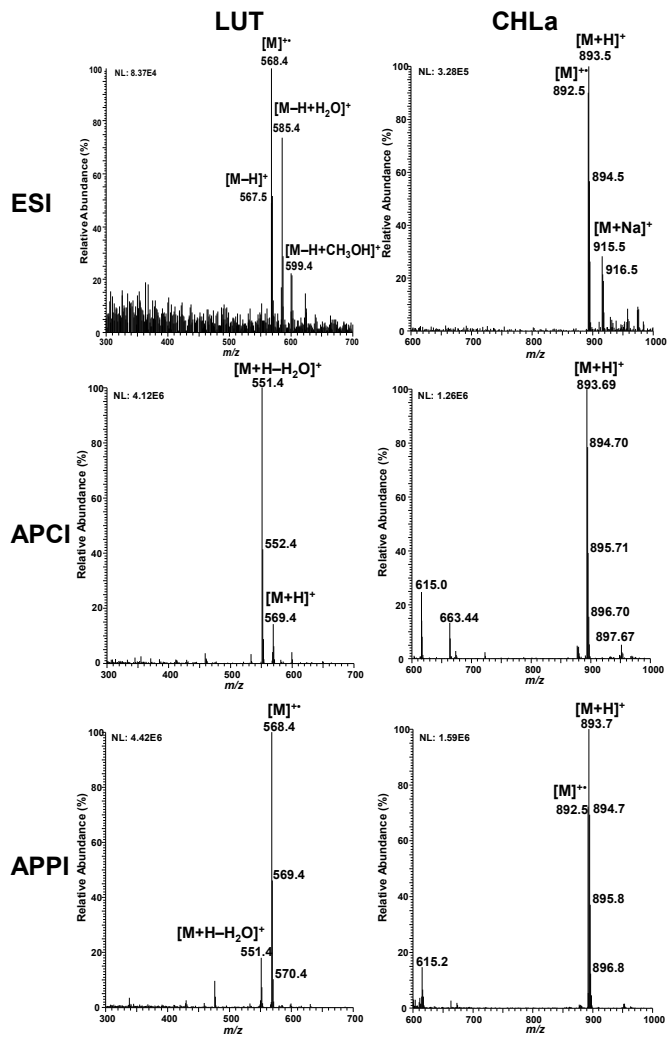
633

634 Figure 3:



635

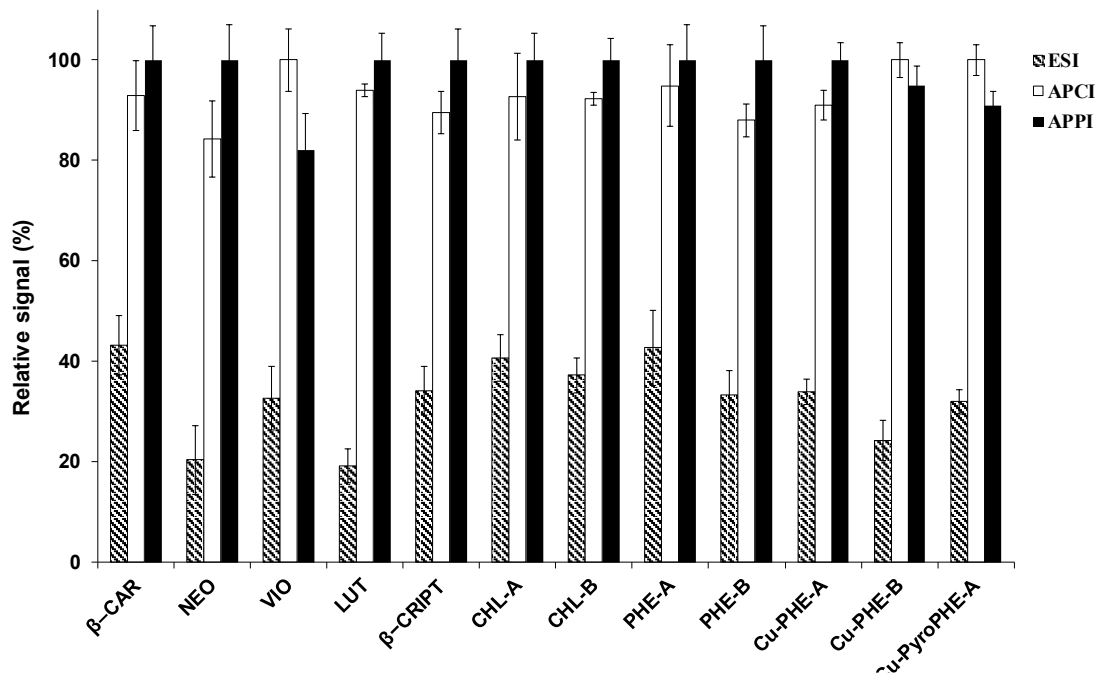
636 Figure 4:



637

638 Figure 5:

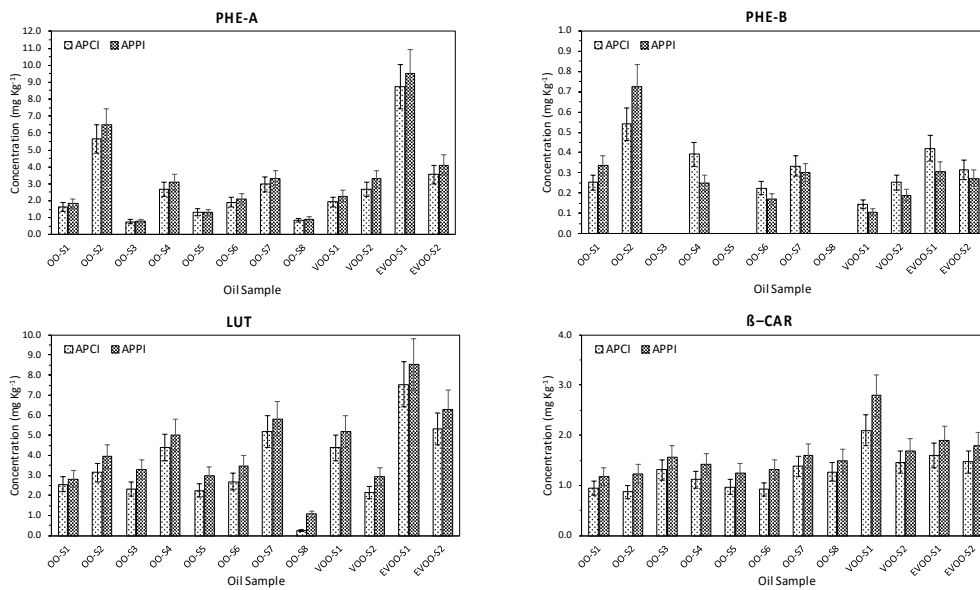
639



640

641

642 Figure 6:

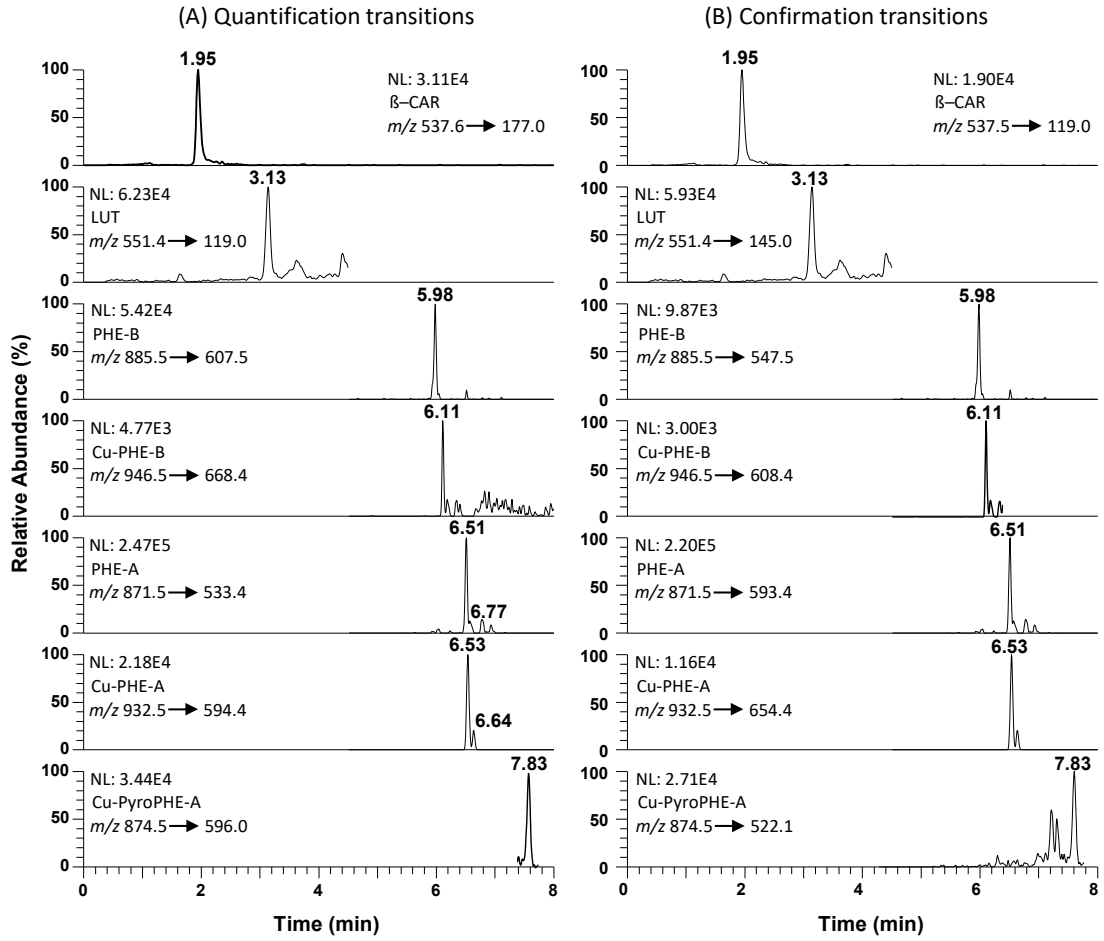


643

644

645

Figure 7:



646

647

**Table 1:** Assignment of ions generated in ESI, APCI and APPI (dopant:chlorobenzene) under optimal conditions

Compound	ESI		APCI		APPI	
	<i>m/z</i> (Rel. Ab. %)	Ion Assignment	<i>m/z</i> (Rel. Ab. %)	Ion Assignment	<i>m/z</i> (Rel. Ab. %)	Ion Assignment
$\beta$ -CAR	536.5 (100)	[M] <sup>+Cl</sup>	537.6 (100)	[M+H] <sup>+</sup>	537.6 (100)	[M+H] <sup>+</sup>
NEO	617.4 (27)	[M-H+H <sub>2</sub> O] <sup>+</sup>	601.4 (67)	[M+H] <sup>+</sup>	600.4 (100)	[M] <sup>+Cl</sup>
	600.4 (100)	[M] <sup>+Cl</sup>	583.4 (100)	[M+H-H <sub>2</sub> O] <sup>+</sup>	583.4 (24)	[M+H-H <sub>2</sub> O] <sup>+</sup>
	599.4 (32)	[M-H] <sup>+</sup>	565.4 (56)	[M+H-2H <sub>2</sub> O] <sup>+</sup>		
VIO	617.4 (27)	[M-H+H <sub>2</sub> O] <sup>+</sup>	601.4 (100)	[M+H] <sup>+</sup>	600.4 (100)	[M] <sup>+Cl</sup>
	600.4 (100)	[M] <sup>+Cl</sup>	583.4 (50)	[M+H-H <sub>2</sub> O] <sup>+</sup>	583.4 (13)	[M+H-H <sub>2</sub> O] <sup>+</sup>
	599.4 (36)	[M-H] <sup>+</sup>				
LUT	599.4 (16)	[M-H+CH <sub>3</sub> OH] <sup>+</sup>	569.4 (18)	[M+H] <sup>+</sup>	568.4 (100)	[M] <sup>+Cl</sup>
	585.4 (75)	[M-H+H <sub>2</sub> O] <sup>+</sup>	551.4 (100)	[M+H-H <sub>2</sub> O] <sup>+</sup>	551.4 (18)	[M+H-H <sub>2</sub> O] <sup>+</sup>
	568.4 (100)	[M] <sup>+Cl</sup>				
	567.4 (53)	[M-H] <sup>+</sup>				
b-CRIPT	583.4 (22)	[M-H+CH <sub>3</sub> OH] <sup>+</sup>	553.4 (100)	[M+H] <sup>+</sup>	553.4 (100)	[M+H] <sup>+</sup>
	552.4 (100)	[M] <sup>+Cl</sup>	535.4 (21)	[M+H-H <sub>2</sub> O] <sup>+</sup>		
	551.4 (13)	[M-H] <sup>+</sup>				
CHL-A	915.6 (27)	[M+Na] <sup>+</sup>	893.5 (100)	[M+H] <sup>+</sup>	893.5 (100)	[M+H] <sup>+</sup>
	893.5 (100)	[M+H] <sup>+</sup>	615.0 (24)	[M+H-C <sub>20</sub> H <sub>38</sub> O <sub>2</sub> ] <sup>+</sup>	892.5 (70)	[M] <sup>+Cl</sup>
	892.5 (88)	[M] <sup>+Cl</sup>				
CHL-B	929.7 (100)	[M+Na] <sup>+</sup>	907.5 (100)	[M+H] <sup>+</sup>	907.5 (100)	[M+H] <sup>+</sup>
	907.5 (26)	[M+H] <sup>+</sup>	629.0 (19)	[M+H-C <sub>20</sub> H <sub>38</sub> O <sub>2</sub> ] <sup>+</sup>	906.5 (50)	[M] <sup>+Cl</sup>
	906.5 (20)	[M] <sup>+Cl</sup>				
PHE-A	871.5 (100)	[M+H] <sup>+</sup>	871.5 (100)	[M+H] <sup>+</sup>	871.5 (100)	[M+H] <sup>+</sup>
	870.5 (85)	[M] <sup>+Cl</sup>	593.0 (20)	[M+H-C <sub>20</sub> H <sub>38</sub> O <sub>2</sub> ] <sup>+</sup>	870.5 (67)	[M] <sup>+Cl</sup>
PHE-B	885.5 (100)	[M+H] <sup>+</sup>	885.5 (100)	[M+H] <sup>+</sup>	885.5 (100)	[M+H] <sup>+</sup>
	884.5 (75)	[M] <sup>+Cl</sup>	607.0 (18)	[M+H-C <sub>20</sub> H <sub>38</sub> O <sub>2</sub> ] <sup>+</sup>	884.5 (62)	[M] <sup>+Cl</sup>
Cu-PHE-A	932.5 (100)	[M+H] <sup>+</sup>	932.5 (100)	[M+H] <sup>+</sup>	932.5 (100)	[M+H] <sup>+</sup>
	931.5 (80)	[M] <sup>+Cl</sup>	654.0 (22)	[M+H-C <sub>20</sub> H <sub>38</sub> O <sub>2</sub> ] <sup>+</sup>	931.5 (67)	[M] <sup>+Cl</sup>

648

649

**Table 2:** Ion assignment of product ions observed in MS/MS using APCI and APPI.

Compound	Ionization source	Precursor ion		Product Ion				
		<i>m/z</i>	Ion Assignment	<i>m/z</i>	Ion Assignment			
β-CAR	APCI/APPI	537.6	[M+H] <sup>+</sup>	177.0	[M+H-C <sub>27</sub> H <sub>36</sub> ] <sup>+</sup>			
				119.0	[M+H-C <sub>31</sub> H <sub>46</sub> ] <sup>+</sup>			
				105.0	[M+H-C <sub>32</sub> H <sub>48</sub> ] <sup>+</sup>			
NEO	APCI	583.4	[M+H-H <sub>2</sub> O] <sup>+</sup>	221.0	[M+H-C <sub>26</sub> H <sub>36</sub> O <sub>2</sub> ] <sup>+</sup>			
				159.0	[M+H-C <sub>28</sub> H <sub>42</sub> O <sub>4</sub> ] <sup>+</sup>			
				119.0	[M+H-C <sub>31</sub> H <sub>46</sub> O <sub>4</sub> ] <sup>+</sup>			
	APPI	600.4	[M] <sup>+□</sup>	145.0	[M-C <sub>29</sub> H <sub>44</sub> O <sub>4</sub> ] <sup>+</sup>			
				171.6	[M-C <sub>27</sub> H <sub>41</sub> O <sub>4</sub> ] <sup>+</sup>			
				119.0	[M-C <sub>31</sub> H <sub>45</sub> O <sub>4</sub> ] <sup>+</sup>			
VIO	APCI	601.4	[M+H] <sup>+</sup>	221.0	[M+H-C <sub>26</sub> H <sub>36</sub> O <sub>2</sub> ] <sup>+</sup>			
				165.0	[M+H-C <sub>30</sub> H <sub>44</sub> O <sub>2</sub> ] <sup>+</sup>			
				119.0	[M+H-C <sub>31</sub> H <sub>46</sub> O <sub>4</sub> ] <sup>+</sup>			
	APPI	600.4	[M] <sup>+□</sup>	145.0	[M-C <sub>29</sub> H <sub>44</sub> O <sub>4</sub> ] <sup>+</sup>			
				171.6	[M-C <sub>27</sub> H <sub>41</sub> O <sub>4</sub> ] <sup>+</sup>			
				119.0	[M-C <sub>31</sub> H <sub>45</sub> O <sub>4</sub> ] <sup>+</sup>			
LUT	APCI	551.4	[M+H-H <sub>2</sub> O] <sup>+</sup>	145.0	[M+H-C <sub>29</sub> H <sub>44</sub> O <sub>2</sub> ] <sup>+</sup>			
				APPI	168.4	[M] <sup>+□</sup>	119.0	[M+H-C <sub>31</sub> H <sub>46</sub> O <sub>2</sub> ] <sup>+</sup>
							105.0	[M+H-C <sub>32</sub> H <sub>48</sub> O <sub>2</sub> ] <sup>+</sup>
b-CRIPT	APCI/APPI	553.4	[M+H] <sup>+</sup>	145.0	[M+H-C <sub>31</sub> H <sub>46</sub> O] <sup>+</sup>			
				119.0	[M+H-C <sub>31</sub> H <sub>46</sub> O] <sup>+</sup>			
				105.0	[M+H-C <sub>30</sub> H <sub>44</sub> O] <sup>+</sup>			
CHL-A	APCI/APPI	893.5	[M+H] <sup>+</sup>	615.5	[M+H-C <sub>20</sub> H <sub>38</sub> ] <sup>+</sup>			
				583.5	[M+H-C <sub>21</sub> H <sub>42</sub> O] <sup>+</sup>			
				555.5	[M+H-C <sub>22</sub> H <sub>42</sub> O <sub>2</sub> ] <sup>+</sup>			
CHL-B	APCI/APPI	907.5	[M+H] <sup>+</sup>	629.5	[M+H-C <sub>20</sub> H <sub>38</sub> ] <sup>+</sup>			
				597.5	[M+H-C <sub>21</sub> H <sub>42</sub> O] <sup>+</sup>			
				569.5	[M+H-C <sub>22</sub> H <sub>42</sub> O <sub>2</sub> ] <sup>+</sup>			
PHE-A	APCI/APPI	871.5	[M+H] <sup>+</sup>	593.4	[M+H-C <sub>20</sub> H <sub>38</sub> ] <sup>+</sup>			
				533.4	[M+H-C <sub>22</sub> H <sub>42</sub> O <sub>2</sub> ] <sup>+</sup>			
PHE-B	APCI/APPI	885.5	[M+H] <sup>+</sup>	607.5	[M+H-C <sub>20</sub> H <sub>38</sub> ] <sup>+</sup>			
				547.5	[M+H-C <sub>22</sub> H <sub>42</sub> O <sub>2</sub> ] <sup>+</sup>			
Cu-PHE-A	APCI/APPI	932.5	[M+H] <sup>+</sup>	654.4	[M+H-C <sub>20</sub> H <sub>38</sub> ] <sup>+</sup>			
				594.4	[M+H-C <sub>22</sub> H <sub>42</sub> O <sub>2</sub> ] <sup>+</sup>			
Cu-PHE-B	APCI/APPI	946.5	[M+H] <sup>+</sup>	668.4	[M+H-C <sub>20</sub> H <sub>38</sub> ] <sup>+</sup>			

650

651



**Table 3:** Quality parameters of UHPLC–MS/MS (APCI and APPI) methods.

Compound	ILOD (mg L <sup>-1</sup> ) <sup>a</sup>		ILOQ (mg L <sup>-1</sup> ) <sup>a</sup>		MLOQ (mg L <sup>-1</sup> ) <sup>a</sup>		Concentration level (mg L <sup>-1</sup> )	Run-to-Run Precision (RSD %)		Trueness (Rel. Error %)	
	APCI	APPI	APCI	APPI	APCI	APPI		APCI	APPI	APCI	APPI
β-CAR	0.03	0.06	0.1	0.2	0.3	0.3	4.5	3	5	4	4
NEO	0.2	0.15	0.8	0.5	0.9	0.6	4.9	2	3	2	3
VIO	0.02	0.03	0.08	0.1	0.1	0.2	4.8	1	1	-1	-0.2
LUT	0.003	0.06	0.01	0.2	0.01	0.2	4.2	1	1	1	3
β-CRIPT	0.1	0.2	0.5	0.6	0.7	0.8	4.6	3	5	-5	-2
CHL-A	0.009	0.021	0.03	0.07	0.05	0.1	4.0	2	2	1	1
CHL-B	0.0009	0.001	0.003	0.004	0.004	0.005	5.0	3	2	3	3
PHE-A	0.01	0.015	0.05	0.05	0.06	0.07	4.3	3	4	-7	-3
PHE-B	0.003	0.006	0.01	0.02	0.03	0.06	4.5	4	2	2	5
Cu-PHE-A	0.009	0.006	0.03	0.02	0.05	0.04	0.2	5	2	10	12
Cu-PHE-B	0.006	0.009	0.02	0.03	0.03	0.05	0.1	5	3	8	6
Cu-PyroPHE-A	0.003	0.006	0.01	0.02	0.03	0.05	0.1	3	7	10	9

<sup>a</sup>Injection volume: 10 μL

652

653

## Supplementary Information

# Simultaneous analysis of natural pigments and E-141i in olive oils by Liquid Chromatography–Tandem Mass Spectrometry

A. Arrizabalaga-Larrañaga<sup>(1)</sup>, P. Rodríguez<sup>(2)</sup>, M. Medina<sup>(2)</sup>, F. J. Santos<sup>(1)</sup>, E. Moyano<sup>(1)\*</sup>

<sup>(1)</sup> Department of Chemical Engineering and Analytical Chemistry, University of Barcelona. Av. Diagonal 645, E-08028 Barcelona, Spain

<sup>(2)</sup> Laboratori Agroalimentari, Generalitat de Catalunya, Vilassar de Mar s/n, 08348 Cabriels, Spain

\* Corresponding author: E. Moyano

## Table of Contents

Supplementary Tables .....	35
<b>Table S1:</b> MRM transitions, optimum collision energies (CE) and ion ratios used in UHPLC–MS/MS. ....	35
<b>Table S2:</b> Assignment of ions observed for CHL-A, $\beta$ -CRIPT, LUT and VIO in APPI using different dopants (post-column addition of 5%, v/v) .....	36
Supplementary Figures.....	4
<b>Figure S1:</b> Effect of vaporizer temperature on the response of VIO in APCI source.....	4
<b>Figure S2:</b> Effect of different dopants (post-column addition of 5% v/v) on the response of some selected photosynthetic pigments using APPI. ....	4
<b>Figure S3:</b> Tandem mass spectrum of Cu-PHE-A using [M+H] <sup>+</sup> as precursor ion. Q1 isolation window: 10 Da FWHM. ....	5
<b>Figure S4:</b> Effect of collision energy (CE) on the response of precursor and product ions for PHE-A and its epimer (PHE-A'). ....	5

682 **Supplementary Tables**683 **Table S1:** MRM transitions, optimum collision energies (CE) and ion ratios used in UHPLC–MS/MS.

Compound	API source	Precursor ion ( <i>m/z</i> )	Quantitation		Confirmation		Ion Ratio $\pm$ SD <sup>a</sup>
			Product ion ( <i>m/z</i> )	CE (eV)	Product ion ( <i>m/z</i> )	CE (eV)	
$\beta$ -CAR	APCI/APPI	537.6	177.0	18	119.0	35	1.6 $\pm$ 0.03
NEO	APCI	583.4	221.0	30	159.0	40	2.2 $\pm$ 0.01
	APPI	600.4	145.0	40	171.6	40	2.3 $\pm$ 0.02
VIO	APCI	601.4	221.0	20	165.0	30	2.9 $\pm$ 0.01
	APPI	600.4	145.0	40	171.6	30	3.0 $\pm$ 0.01
LUT	APCI	551.4	119.0	40	145.0	40	1.1 $\pm$ 0.01
	APPI	568.4	145.0	35	119.0	45	1.1 $\pm$ 0.01
$\beta$ -CRIPT	APCI/APPI	553.4	119.0	40	105.4	45	1.6/1.6 $\pm$ 0.02
CHL-A	APCI/APPI	893.5	555.5	40	615.5	20	1.7/1.8 $\pm$ 0.01
CHL-B	APCI/APPI	907.5	629.5	25	569.5	25	1.8/1.8 $\pm$ 0.02
PHE-A	APCI/APPI	871.5	533.4	50	593.4	45	1.1/1.1 $\pm$ 0.03
PHE-B	APCI/APPI	885.5	607.5	35	547.5	45	1.1/1.2 $\pm$ 0.02
Cu-PHE-A	APCI/APPI	932.5	594.4	40	654.4	25	1.9/1.9 $\pm$ 0.05
Cu-PHE-B	APCI/APPI	946.5	668.4	25	608.4	25	1.6/1.7 $\pm$ 0.07
Cy-PyropHE-A	APCI/APPI	874.5	595.0	25	522.1	30	1.3/1.2 $\pm$ 0.06

684 <sup>a</sup>SD, standard deviation (n:5)

685

686 **Table S2:** Assignment of ions observed for CHL-A,  $\beta$ -CRIPT, LUT and VIO in APPI using different dopants (post-column addition of 5%, v/v)

Pigment	$m/z$	Ion Assignment	No - dopant	Dopant		
			Rel. Ab. %	Acetone Rel. Ab. %	THF Rel. Ab. %	Toluene Rel. Ab. %
VIO	601.4	[M+H] <sup>+</sup>	100	100	100	100
	583.4	[M+H-H <sub>2</sub> O] <sup>+</sup>	85	55	60	60
	565.4	[M+H-2·H <sub>2</sub> O] <sup>+</sup>	18	10	10	10
LUT	551.4	[M+H-H <sub>2</sub> O] <sup>+</sup>	100	100	100	100
$\beta$ -CRIPT	553.4	[M+H] <sup>+</sup>	100	100	100	100
	535.4	[M+H-H <sub>2</sub> O] <sup>+</sup>	22	33	11	27
CHL-A	893.5	[M+H] <sup>+</sup>	100	100	100	100

Pigment	$m/z$	Ion Assignment	Dopant	
			Anisole Rel. Ab. %	Chlorobenzene Rel. Ab. %
VIO	600.4	[M] <sup>+•</sup>	100	100
	583.4	[M+H-H <sub>2</sub> O] <sup>+</sup>	5	12
LUT	568.4	[M] <sup>+•</sup>	100	100
	551.4	[M+H-H <sub>2</sub> O] <sup>+</sup>	14	18
$\beta$ -CRIPT	553.4	[M+H] <sup>+</sup>	100	100
CHL-A	893.5	[M+H] <sup>+</sup>	100	100
	892.5	[M] <sup>+•</sup>	85	77

687

## Supplementary Figures

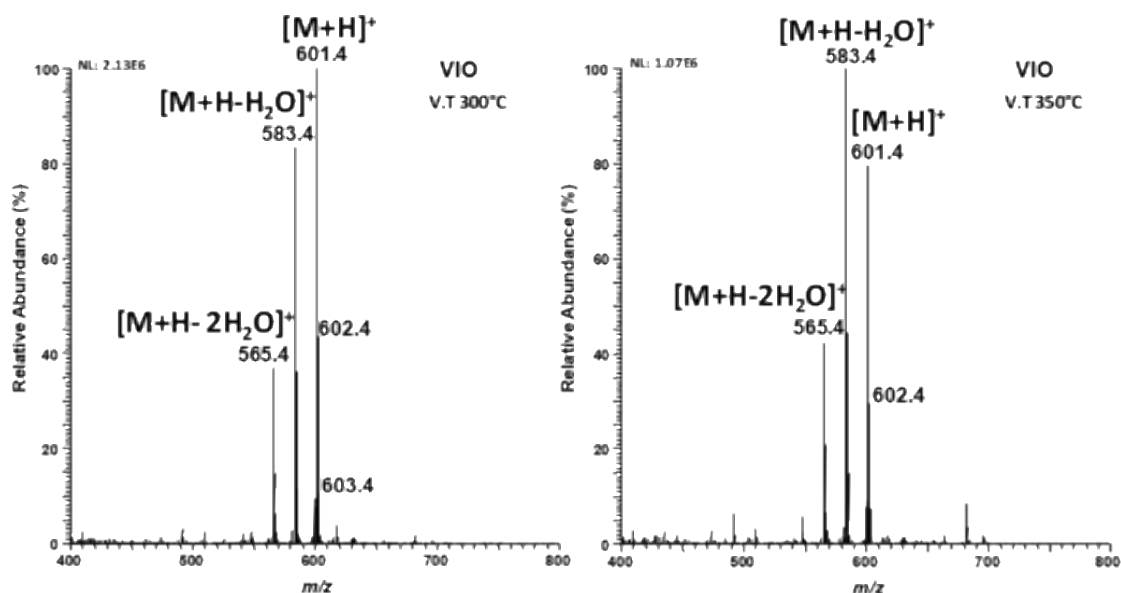


Figure S1: Effect of vaporizer temperature on the response of VIO in APCI source.

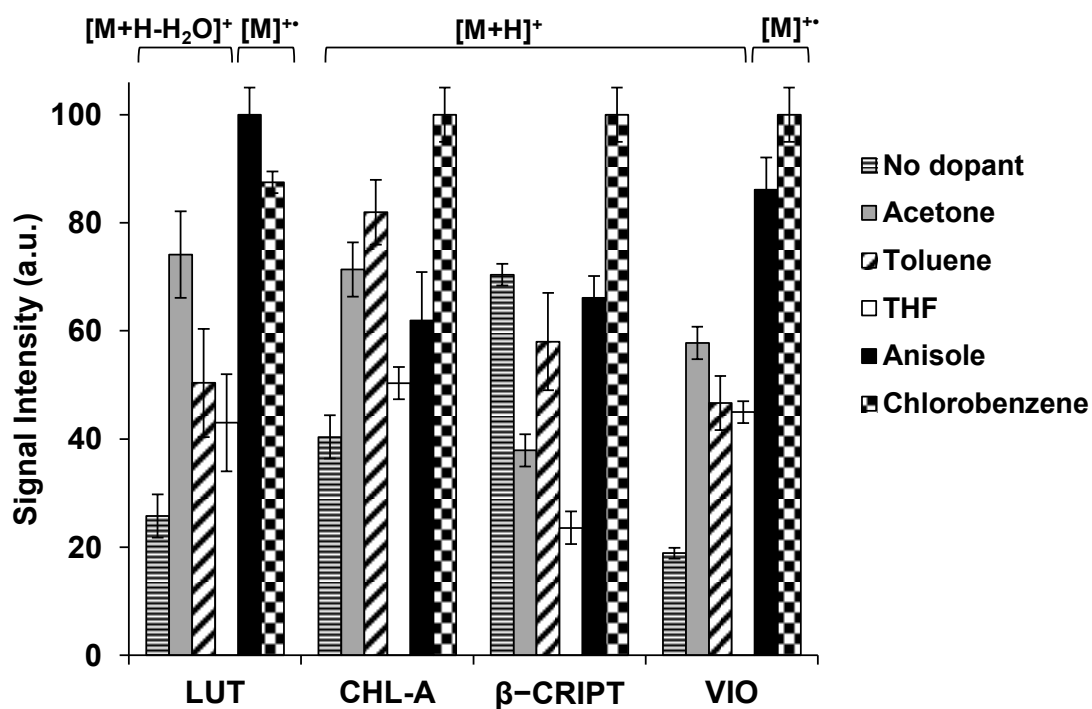
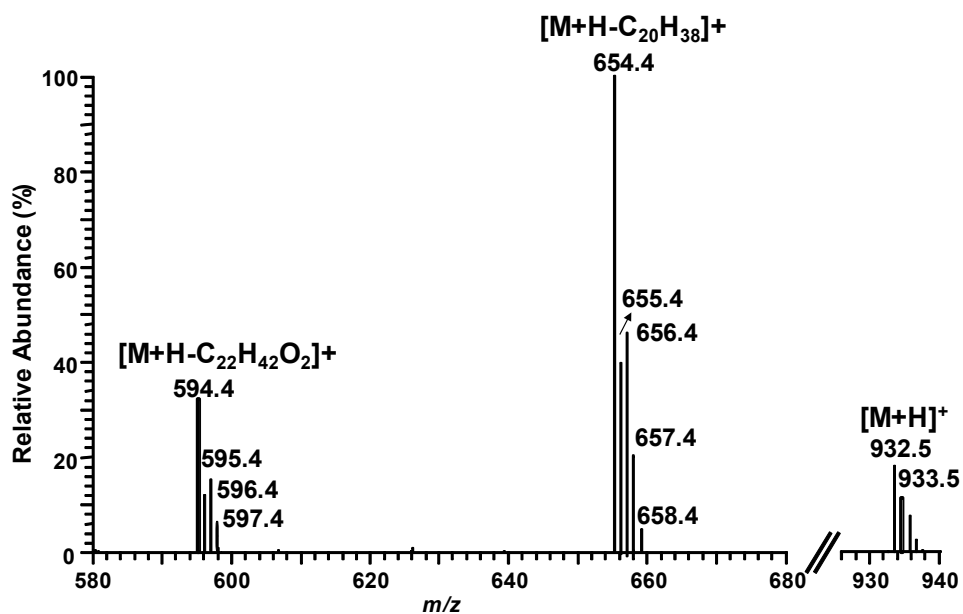


Figure S2: Effect of different dopants (post-column addition of 5% v/v) on the response of some selected photosynthetic pigments using APPI.

688

689



**Figure S3:** Tandem mass spectrum of Cu-PHE-A using  $[M+H]^+$  as precursor ion. Q1 isolation window: 10 Da FWHM.

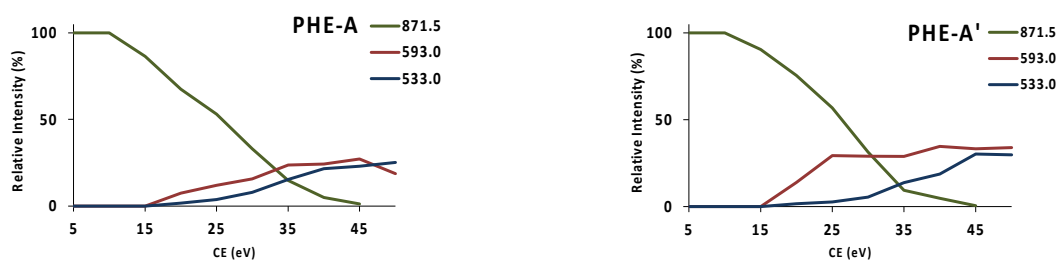


**Figure S4:** Effect of collision energy (CE) on the response of precursor and product ions for PHE-A and its epimer (PHE-A').